

## Photoelectric properties and photocatalytic activity of silver-coated titanium dioxides

C. Damm<sup>a,\*</sup>, G. Israel<sup>b</sup>

<sup>a</sup> *Friedrich-Alexander-University Erlangen-Nuremberg, Institute of Polymer Materials, Martensstrasse 7, D-91058 Erlangen, Bavaria, Germany*

<sup>b</sup> *Martin-Luther-University Halle-Wittenberg, Institute of Organic Chemistry, Kurt-Mothes-Strasse 2, D-06120 Halle/Saale, Germany*

Received 21 June 2006; received in revised form 2 July 2006; accepted 3 July 2006

Available online 28 August 2006

### Abstract

Silver was deposited onto the surface of different commercial titanium dioxides namely, the pigment “K1001” and the two photocatalysts “P-25” and “Hombikat-UV”. Both the coated and the untreated materials were used as catalysts for the heterogeneous photocatalytic initiation of the photopolymerisation of an ethoxylated trisacrylate. The coated pigment “K1001-Ag” more effectively initiated acrylate polymerisation than the untreated material exhibiting only small photocatalytic activity. In contrast, the deposition of silver on the photocatalysts affected their photocatalytic activity detrimentally; in the presence of “P-25-Ag” after 120 s illumination, only 10% of the monomer was polymerised. In the presence of “Hombikat-UV-Ag” no photopolymerisation was observed.

Transient photo-EMF measurements revealed that the photoelectric properties of the materials are influenced by silver deposition. The efficiency of charge separation and the charge carrier lifetime in the surface region of “K1001” increased slightly as a result of silver deposition. Contrary to that, silver lowered the efficiency of charge separation and the charge carrier lifetime in the surface region of “P-25” and “Hombikat-UV”.

Substrate-dependent morphology of the deposited silver particles seems to be the reason for the different effect of silver. Diffuse reflection spectra of “P-25-Ag” and “Hombikat-UV-Ag” show an absorption peak in the spectral region of the surface plasmon resonance of silver nanoparticles, whereas “K1001-Ag” exhibits a nearly continuous absorption in the visible range while speaking for silver micro- and submicroparticles.

© 2006 Elsevier Ltd. All rights reserved.

**Keywords:** Titanium dioxide; Silver; Photopolymerisation; Photo-EMF

### 1. Introduction

The main application of titanium dioxide photocatalysis is the purification of wastewater and air [1–3]. In this process organic pollutants are oxidatively degraded and, after several reaction steps, are completely mineralised. Moreover, by applying suitable electron donors, noble metal salts can be photocatalytically reduced to metals and deposited on the surface of titanium dioxide. Such reductive processes can be used for the recovery of noble metals from wastewater [4–6]. The

noble metal-modified titanium dioxide photocatalysts that result from this reductive process are interesting materials in the context of heterogeneous photocatalysis. Many papers have revealed that the deposition of noble metal enhances the photocatalytic activity of titanium dioxide. For example, platinized titanium dioxide was shown to be a very active photocatalyst for hydrogen generation due to water splitting [7].

Silver-coated titanium dioxide photocatalysts have also been investigated by many researchers [8–12] which showed [12] that the morphology of the deposited silver particles depends on the type of titanium dioxide used as substrate material.

Many workers have observed enhanced degradation rates of dyes due to the deposition of silver on titanium dioxide [10,11]. Sung-Suh et al. [10] showed that silver-modified

\* Corresponding author. Tel.: +49 9131 85 27748; fax: +49 9131 85 28321.

E-mail address: [Cornelia.damm@ww.uni-erlangen.de](mailto:Cornelia.damm@ww.uni-erlangen.de) (C. Damm).

titanium dioxide was able to degrade dyes under illumination with visible light only.

Besides heterogeneous photocatalysis of silver-modified titanium dioxide is interesting because of its antimicrobial properties [13].

Heterogeneous photocatalytic polymerisation reactions on silver-coated titanium dioxides could be a convenient way for the preparation of antimicrobial coatings. But up to now little is known about heterogeneous photocatalytic initiation of polymerisations. In Refs. [14,15] it was shown that the ability of titanium dioxide to initiate an acrylate polymerisation can be enhanced or decreased by doping with metal ions [15] as well as with nonmetals [14] or by coating with inorganic semiconductors [15].

In this paper we report about the heterogeneous photocatalysed polymerisation of an ethoxylated trisacrylate using silver-coated titanium dioxides as photocatalysts. The initiation behaviour of the silver-coated samples is compared with that of the neat materials.

The first step of any photocatalytic reaction is the formation and separation of electrons and holes in the photocatalyst material under illumination. Thus the photoelectric properties of the catalyst material are essential for its photocatalytic activity. A high efficiency of charge separation and a sufficient long lifetime of the charge carriers in the surface region of the catalyst material are the necessary preconditions for a good photocatalytic activity.

Noble metals are known to form Schottky-barriers at the surface of titanium dioxide [16]. Thus they trap electrons and in this way the charge separation is facilitated. Consequently, the deposition of noble metals alters the photoelectric properties of titanium dioxide.

The enhanced photocatalytic activity of noble metal-modified titanium dioxide photocatalysts is usually explained on the basis of the photoelectric properties of the catalyst materials. But mostly the photoelectric properties of the catalysts are not measured.

In this paper the polymerisation attempts are combined with the characterisation of the photoelectric properties of the silver-coated and the neat-titanium dioxides. For that measurements of the transient photo-EMF are used because this method records the photovoltage contactless and without any external electric field. Thus the charge carrier concentration gradient due to the gradient of light absorption as well as surface states, impurity places and heterojunctions are the only driving forces for a photo-EMF generation. For that reason the photo-EMF parameters do excellent reflect the structural properties of the photoconductor samples.

The photo-EMF signals of the samples investigated start with a positive sign and show a zero potential passage. Such signals are typical for n-type photoconductors.

The amount of the maximum photo-EMF,  $U_{\max}$ , upon illumination is a measure of the efficiency of charge generation and separation in competition to deactivation processes due to recombination or chemical reactions of the charge carriers. For the description of the photo-EMF decay a biexponential rate law is used, see Eq. (1).

$$U(t) = U_1^0 \exp(-k_1 t) + U_2^0 \exp(-k_2 t) \quad (1)$$

As per definition, the process with the parameters  $U_1^0$  and  $k_1$  is always a faster decay process. That means  $k_1 > k_2$ .

The cause of the biexponential decay behaviour of the photo-EMF is the generation of two partial photo-EMFs decaying independently. The partial voltages  $U_1^0$  and  $U_2^0$  are the values of both photo-EMFs at the beginning of their decay process with  $k_1$  and  $k_2$  as their first order decay constants. The sum of  $U_1^0$  and  $U_2^0$  is  $U_{\max}$ .

In a previous work it was shown that the generation of a photo-EMF in the subsurface region additional to the Dember-EMF in the bulk causes the biexponential photo-EMF decay. According to the findings of our previous works we are able to assign the faster decay process (parameters  $U_1^0$ ,  $k_1$ ) to a photo-EMF in the subsurface region of the catalyst particles [17,18]. That means  $U_1^0$  represents a charge carrier amount in the subsurface region,  $k_1$  is a measure of the recombination rate in the surface/subsurface region. So the charge carrier lifetime in the surface region  $\tau_{CC}$  which is essential for heterogeneous photocatalysis can be derived from  $k_1$ :  $\tau_{CC} = 1/k_1$ .

In Ref. [18], the photo-EMF method is described more in detail.

## 2. Experimental

### 2.1. Materials

The base materials were of uncoated  $\text{TiO}_2$  pigment grade K1001 made by Kronos as well as  $\text{TiO}_2$  photocatalysts “P-25” (Degussa) and “Hombikat-UV” (Sachtleben chemistry).

Silver nitrate, 0.1 N nitric acid, sodium borohydride, 1, 2-dichlorethane and dichloromaleic acid anhydride were purchased from Merck. The pigments and chemicals mentioned above were used as received. The acrylate used (grade SR415) was purchased from Cray Valley; prior to use, the inhibitors were removed by filtration over an  $\text{Al}_2\text{O}_3$  column.

### 2.2. Preparation of silver-modified titanium dioxides

Twenty-one milligrams ( $1.25 \times 10^{-4}$  mol) of silver nitrate was dissolved in 400 ml of distilled water. One gram ( $1.25 \times 10^{-2}$  mol) of the titanium dioxide powder was dispersed in this solution under stirring. The pH of the dispersion was adjusted to 2 using 0.1 N nitric acid to avoid the deposition of silver oxide on the surface of titanium dioxide grains.

After 24 h of stirring at room temperature no silver ions could be detected in the supernatant by means of anodic stripping voltammetry. That means the silver ions present in the solution were completely adsorbed on the titanium dioxide, but no colour change of the solid was observed.

The silver ions adsorbed on titanium dioxide were reduced to elemental silver by dropwise addition of the calculated amount of a freshly prepared  $10^{-3}$  N aqueous solution of sodium borohydride to the dispersion. Immediately after the

addition of the reduction agent a colour change of the solid was observed.

### 2.3. Structural analyses

Powder X-ray diffraction (XRD) patterns were recorded in the range from 10° to 70° (X'Pert Pro MPD, Cu K $\alpha$  radiation, Philips).

The specific surface areas were determined by the BET method (N<sub>2</sub> adsorption).

Diffuse reflection spectra of powders were recorded using a Shimadzu UV-2401, UV/vis spectrophotometer equipped with a diffuse reflectance accessory. BaSO<sub>4</sub> was used as a white standard.

The morphology of the titanium dioxide powders was investigated by high-resolution scanning electron microscopy (SEM) (Zeiss).

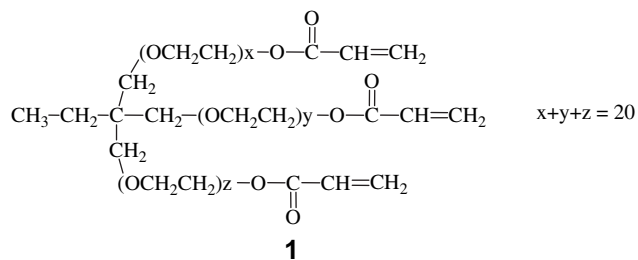
### 2.4. Photo-EMF measurements

Photo-EMF measurements were performed using pigment polymer dispersion films (polymeric binder: polyvinyl butyral, film thickness: 60–80  $\mu$ m, total absorption in the UV range). For details of sample preparation see Ref. [18]. Circular samples of 10 mm diameter were cut from the films and transferred into the photo-EMF device which is constructed like a capacitor containing one transparent electrode. The sample was illuminated by a single flash of a nitrogen laser PNL 100; Lasertechnik Berlin GmbH (wavelength: 337 nm, pulse duration: 300 ps, power: 100 kW) through the transparent electrode. The energy of the actinic light pulse arriving at the sample was about  $3 \times 10^{13}$  quanta per flash. Temperature of sample and amplifier was 25 °C. All photo-EMF signals and parameters reported in this paper are the mean values of three measurements. Each measurement was performed using a new sample.

The photo-EMF device is described more in detail in Ref. [18].

### 2.5. Photopolymerisation

The light induced polymerisation of the trisacrylate **1** was performed in the presence of 5.5 wt% of the titanium dioxide powder and 6.5 mol% (rel. to **1**) of dichloromaleic acid anhydride (DCMA) as electron acceptor.



To disperse the powder in the monomer, a one ball vibrat-mill was used. A 20  $\mu$ m thick film of the pigment–monomer mixture was produced on the ATR crystal of the IR

spectrometer by pasting with the help of a knife coater. The white light of a 100-W mercury high pressure lamp was focused on the surface of the ATR crystal (2 mm  $\times$  2 mm). To avoid a direct excitation of the acrylate monomer, all radiations below 350 nm were removed through a corresponding cut-off glass filter (Schott). Light intensity arriving at the sample surface was 37 mW/cm<sup>2</sup>. The relative concentration of double bonds was determined by real-time infrared spectroscopy (ATR-FTIR) with a “FTS6000” (Biorad) spectrometer monitoring the absorption band at 810 cm<sup>−1</sup> (C=C–H wagging vibration) of the acrylate monomer as a function of the illumination time. To exclude oxygen the sample chamber of the spectrometer was flushed with nitrogen 3 min before as well as during the entire irradiation experiment. The results of all polymerisation experiments are mean values of three experiments. The ATR-FTIR apparatus is described in more detail in Ref. [19].

## 3. Results and discussion

### 3.1. Structure of the photocatalyst materials

According to our XRD investigations and to the suppliers' information, the pigment “K1001” and the photocatalyst “Hombikat-UV” are anatase-type titanium dioxides. The photocatalyst “P-25” consists of about 85% anatase and 15% rutile.

From the line width of the (101) diffraction peak of the anatase polymorph at  $2\theta = 25.3^\circ$  and the (110) peak of the rutile polymorph at  $2\theta = 27.4^\circ$ , the primary crystallite sizes summarized in Table 1 were calculated using the Scherrer equation.

All the titanium dioxides investigated in this work are nanocrystalline materials. The pigment “K1001” consists of much larger primary crystallites than the photocatalysts “P-25” and “Hombikat-UV”.

The XRD spectra of the silver-coated materials do not show any additional diffraction peak although silver is a crystalline material. That means the silver content of the coated titanium dioxides is too low to be detected by XRD.

In Fig. 1a–c, SEM micrographs of the coated titanium dioxides are displayed.

All the materials investigated consist of aggregates and agglomerates of spherical primary particles, having diameters in the size range from about 100 nm to about 200 nm, cf. Fig. 1a–c. Nevertheless, the specific surface areas of the three materials are strongly different, cf. Table 1. Comparing the results shown in Table 1 and from Fig. 1a–c, it can be concluded that the size of aggregates and agglomerates

Table 1  
Particle properties of the titanium dioxides investigated

TiO <sub>2</sub> sample	Polymorph	Primary crystallite size/nm	Specific surface area/m <sup>2</sup> $\times$ g <sup>−1</sup>
K1001	Anatase	62	11
P-25	85% Anatase	19 (anatase)	50
	15% Rutile	30 (rutile)	
Hombikat-UV	Anatase	14	>300

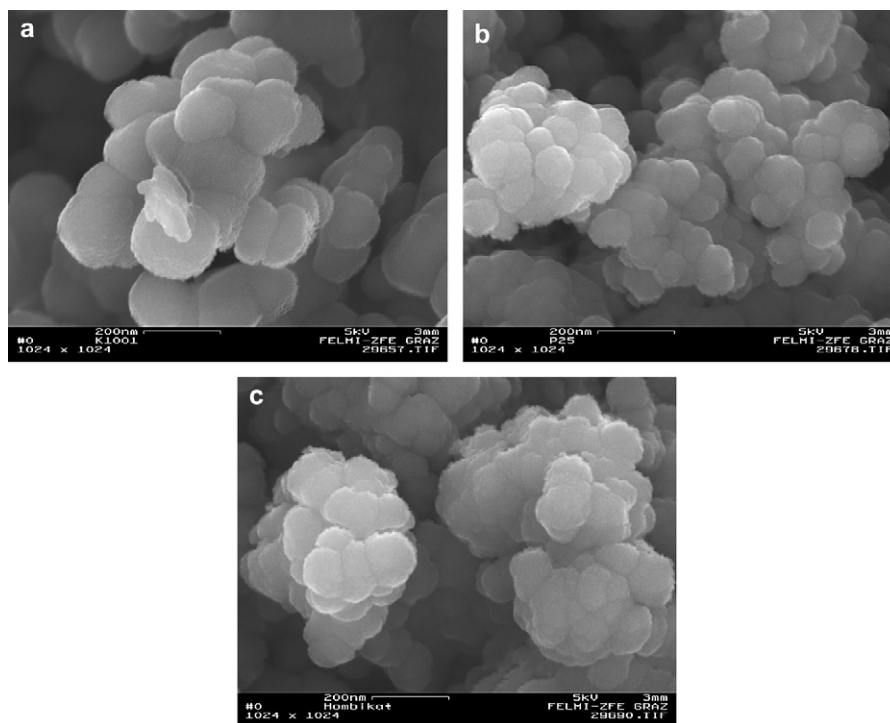


Fig. 1. SEM micrographs of: (a) silver-coated titanium dioxide pigment “K1001-Ag”, (b) silver-coated titanium dioxide photocatalyst “P-25-Ag”, and (c) silver-coated titanium dioxide photocatalyst “Hombikat-UV-Ag”.

must increase in the following direction: “Hombikat-UV” < “P-25” < “K1001”.

In the SEM micrographs shown in Fig. 1a–c only titanium dioxide particles can be seen although the coated materials are coloured being a proof for the presence of the silver. Thus it can be concluded that either the amount of silver particles is too low, so that the probability to find a silver particle in SEM is small, or that the size of the silver particles is too small, so that the resolution of SEM is not sufficient to detect them.

According to Ref. [20] there is a relationship between the colour and the size and shape of metallic nanoparticles. Thus diffuse reflection spectra of the coated materials can yield valuable information about the morphology of the silver particles on the surface of the titanium dioxides, cf. Fig. 2.

The silver-coated titanium dioxide pigment “K1001-Ag” shows a nearly continuous absorption in the visible spectral range, see curve 1 in Fig. 2. This absorption feature is typical for “normal” silver particles having sizes in the micrometer or submicrometer range.

In contrast, the coated photocatalysts show an absorption peak in the visible range. The peak location amounts to about 430 nm for “Hombikat-UV-Ag” (cf. curve 3 in Fig. 2) and about 525 nm for “P-25-Ag” (cf. curve 2 in Fig. 2), respectively. According to Ref. [20], an absorption peak between 400 and 450 nm corresponds to the surface plasmon resonance absorption of silver nanoparticles. If the silver nanoparticles form small aggregates, then the absorption maximum due to the surface plasmon resonance phenomenon is shifted bathochromically [20]. Thus it can be assumed that small aggregates of silver nanoparticles are present on the surface of “P-25”.

Comparing the absorption spectra of the coated titanium dioxides (Fig. 2) with the particle properties of the base materials (Table 1), it becomes clear that the size of the deposited silver particles decreases with increasing specific surface area of the carrier.

### 3.2. Photoelectric properties

The photo-EMF signals of the neat- and the silver-coated titanium dioxides displayed in Fig. 3a and b were evaluated

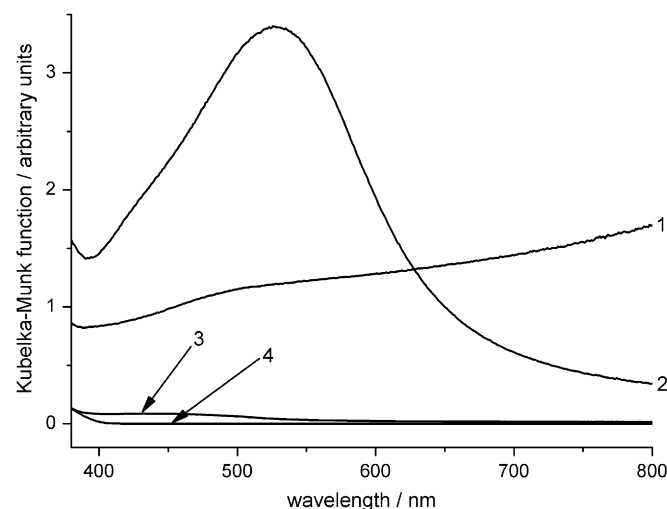


Fig. 2. Powder absorption spectra of the silver-coated titanium dioxides; curve 1: “K1001-Ag”; curve 2: “P-25-Ag”; curve 3: “Hombikat-UV-Ag”. The neat “K1001”, “P-25” and “Hombikat-UV” do not show any absorption in the visible spectral range (curve 4).



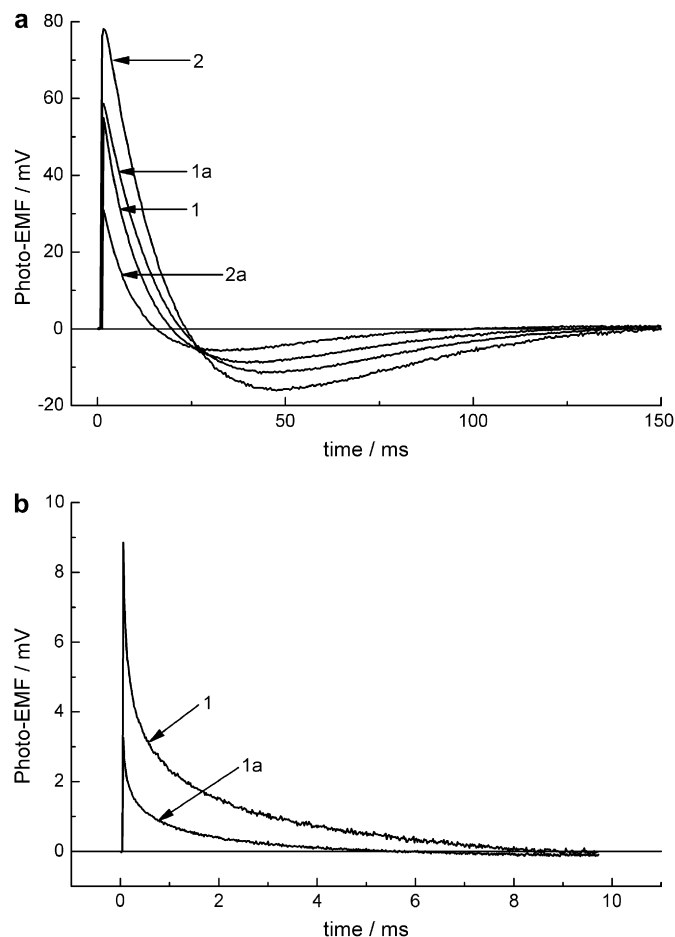


Fig. 3. Photo-EMF signals of (a) the pigment “K1001” (curve 1), the photocatalyst “P-25” (curve 2), the silver-coated pigment “K1001-Ag” (curve 1a) and the silver-coated photocatalyst “P-25-Ag” (curve 2a). (b) Photo-EMF signals of the neat (curve 1) and the silver-coated (curve 1a) photocatalyst “Hombikat-UV”.

by Eq. (1). From the rate constant  $k_1$  the charge carrier lifetime in the surface region  $\tau_{CC}$  was calculated by  $\tau_{CC} = 1/k_1$ .

Moreover the maximum photo-EMF  $U_{max}$  being a relative measure of the efficiency of charge separation was taken from the experimental curves shown in Fig. 3a and b.

Among the neat-titanium dioxide samples, the photocatalyst “P-25” exhibits the largest maximum photo-EMF  $U_{max}$ , cf. Table 1. That means due to the anatase-rutile heterostructure the charge separation in “P-25” is more efficient than in the pure anatase materials. Moreover the charge carrier lifetime in the surface region of “P-25” is longer than in the other materials. Thus, according to the photoelectric properties, among the neat materials “P-25” should have the best photocatalytic activity.

The pigment “K1001” does also show a fairly high efficiency of charge separation and a sufficient long charge carrier lifetime in the surface region. For these reasons “K1001” should also be a photocatalytic active material.

In contrast, the maximum photo-EMF of “Hombikat-UV” is about one order of magnitude and the charge carrier lifetime is two orders of magnitude smaller in comparison to the other

titanium dioxides, cf. Table 1. Thus, for “Hombikat-UV” only a medium photocatalytic activity is expected although it has a much larger specific surface area than the other titanium dioxides.

The deposition of silver influences the photoelectric properties of all titanium dioxides investigated strongly, cf. Table 1.

The efficiency of charge separation and the charge carrier lifetime in the pigment “K1001” are slightly increased due to coating with silver. Such behaviour was expected, because it is known that titanium dioxide/silver Schottky heterojunctions facilitate charge separation and push the electron/hole recombination back [16].

According to the photoelectric properties, the silver-coated pigment “K1001-Ag” should exhibit a higher photocatalytic activity than the neat one.

In contrast to the pigment “K1001”, the deposition of silver onto the photocatalysts “P-25” and “Hombikat-UV” leads to a decrease of the maximum photo-EMF by about a factor of 2, cf. Table 2. Moreover the charge carrier lifetime in these materials becomes shorter due to coating with silver. These findings prove that the silver particles present on the surface of the photocatalysts “P-25” and “Hombikat-UV” facilitate the electron/hole recombination. Thus for “P-25” and “Hombikat-UV” one should expect that silver coating has a detrimental effect on the photocatalytic activity.

### 3.3. Photopolymerisation

The photopolymerisation of the ethoxylated trisacrylate **1** was chosen as a test reaction to check the hypotheses stated in Section 3.2.

The kinetic curves shown in Fig. 4 resulting from monomer disappearance were differentiated to obtain monomer conversion rates  $r_P$  which were plotted versus the relative monomer concentration. Except at very early reaction stages (corresponding to an induction period) a linear relationship between  $r_P$  and the relative monomer concentration was observed indicating a first order polymerisation process, as expected for a free radical polymerisation. From the slope of the  $r_P$ –monomer concentration plots the polymerisation rate constant  $K$  was determined. The values for  $K$  as well as for the maximum polymerisation rate  $r_P^{max}$  are summarized in Table 3.

Table 2

Maximum photo-EMF,  $U_{max}$ , and charge carrier lifetime in the surface region,  $\tau_{CC}$ , of the neat- and silver-coated titanium dioxides

TiO <sub>2</sub> sample	Maximum photo-EMF, $U_{max}$ /mV	Charge carrier lifetime in the surface region, $\tau_{CC}$ /ms
K1001	$54.9 \pm 2.8$	$20 \pm 0.8$
K1001-Ag	$58.8 \pm 2.0$	$23 \pm 0.7$
P-25	$78.1 \pm 2.1$	$24 \pm 0.5$
P-25-Ag	$31.4 \pm 0.9$	$16 \pm 0.4$
Hombikat-UV	$7.6 \pm 1.0$	$0.11 \pm 0.03$
Hombikat-UV-Ag	$2.9 \pm 0.6$	$0.07 \pm 0.01$

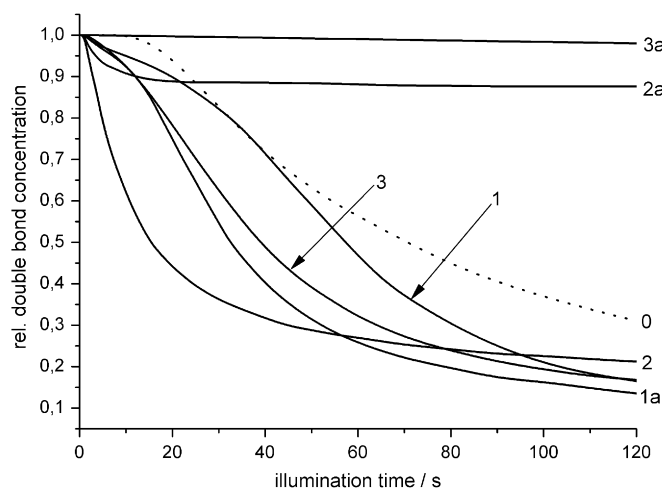


Fig. 4. Kinetics of the photopolymerisation of the acrylate **1** pigmented with 5.5 wt% of the  $\text{TiO}_2$  samples mentioned (solid lines): curve 1: “K1001”, curve 1a: “K1001-Ag”, curve 2: “P-25”, curve 2a: “P-25-Ag”, curve 3: “Hombikat-UV”, and curve 3a: “Hombikat-UV-Ag”. The dotted line shows the polymerisation kinetics of the acrylate without  $\text{TiO}_2$  but in the presence of the electron acceptor dichloromaleic acid anhydride (curve 0).

The neat photocatalysts “P-25” (curve 2 in Fig. 4) and “Hombikat-UV” (curve 3 in Fig. 4) as well as the untreated pigment “K1001” (curve 1 in Fig. 4) accelerate the photopolymerisation of the acrylate **1** by their photocatalytic activity. As expected from the results of the photo-EMF studies in the presence of neat “P-25” the highest polymerisation rate is observed. The photocatalyst “Hombikat-UV” exhibits only a medium activity although its specific surface area is much larger than that of “P-25”.

In comparison to the pigment “K1001”, the specific surface area of the photocatalyst “Hombikat-UV” is larger by a factor of 27, but the polymerisation rate constant  $K$  is higher only by a factor of 1.2.

From these findings it becomes obvious that for an efficient initiation of a photopolymerisation, not only the specific surface area but also suitable photoelectric properties of the catalyst material are very important.

As expected the ability of the titanium dioxides to initiate a photopolymerisation of **1** is influenced by coating with silver. Indeed, the silver-coated pigment “K1001-Ag” (curve 1a in Fig. 4) initiates the polymerisation of **1** noticeably better than the neat one. Among the silver-coated materials “K1001-Ag” exhibits the highest photocatalytic activity.

Table 3  
Maximum rate of the photopolymerisation,  $r_p^{\max}$ , and photopolymerisation rate constant,  $K$ , of the acrylate samples mentioned in Fig. 4

$\text{TiO}_2$ sample	Maximum polymerisation rate, $r_p^{\max}/\text{s}^{-1}$	Polymerisation rate constant, $K/\text{s}^{-1}$
Without $\text{TiO}_2$ (reference)	$(1.18 \pm 0.12) \times 10^{-2}$	$(1.80 \pm 0.09) \times 10^{-2}$
K1001	$(1.30 \pm 0.13) \times 10^{-2}$	$(2.65 \pm 0.25) \times 10^{-2}$
K1001-Ag	$(2.07 \pm 0.21) \times 10^{-2}$	$(3.67 \pm 0.21) \times 10^{-2}$
P-25	$(6.00 \pm 0.60) \times 10^{-2}$	$(8.94 \pm 0.38) \times 10^{-2}$
P-25-Ag	$(3.20 \pm 0.32) \times 10^{-2}$	$(5.05 \pm 0.22) \times 10^{-2}$
Hombikat-UV	$(1.62 \pm 0.16) \times 10^{-2}$	$(3.11 \pm 0.15) \times 10^{-2}$
Hombikat-UV-Ag	$\approx 0$	$\approx 0$

The detrimental effect of silver in “P-25” and “Hombikat-UV” predicted by the photo-EMF measurements is really observed.

“Hombikat-UV-Ag” inhibits the photopolymerisation of **1** completely, cf. curve 3a in Fig. 4. That means it does not show any photocatalytic activity but it suppresses the homogenous polymerisation of the acrylate by acting as a light filter.

In the presence of “P-25-Ag” at the beginning of the polymerisation process a fairly high polymerisation rate is observed, cf. Table 3. But the polymerisation rate decreases very fast and after about 20 s illumination the polymerisation process stops, cf. curve 2a in Fig. 4. After 120 s illumination only about 10% of the monomer was converted in the presence of “P-25-Ag” whereas about 80% monomer conversion was achieved in the presence of neat “P-25”. Even in the absence of any titanium dioxide under otherwise the same conditions 70% monomer conversion are achieved after 120 s illumination. These findings prove that “P-25-Ag” does not show a noticeable photocatalytic activity.

#### 4. Conclusions

The photoelectric properties as well as the photocatalytic activity of titanium dioxides can be modified by deposition of silver. The effect of silver depends on carrier material: The photocatalytic activity of the titanium dioxide pigment “K1001” was noticeably improved by coating with silver. The reason for that is a slight increase of the efficiency of charge separation and an enhanced charge carrier lifetime which can be explained by Schottky heterojunctions.

In contrast, silver deposition has a negative effect on the photocatalytic activity of the photocatalysts “P-25” and “Hombikat-UV” because it shortens the charge carrier lifetime in the surface region and it causes a decrease of the efficiency of charge separation. The reason for that seems to be the particle size of the silver deposit. The powder absorption spectra give hints that on “P-25” and on “Hombikat-UV” silver nanoparticles were formed, whereas on the pigment “K1001” micro and submicroparticles were precipitated.

Generally it was shown in this work that photo-EMF measurements are a valuable tool to predict whether a material is photocatalytic active or not.

Moreover it was proven that in the presence of the silver-coated titanium dioxide pigment “K1001-Ag” a satisfying acrylate photopolymerisation rate is observed. Thus “K1001-Ag” may be used for the preparation of antimicrobial coatings by means of heterogeneous photocatalytic polymerisation, which means in the absence of classical molecular photoinitiators.

#### Acknowledgements

The authors are grateful to the German Research Foundation (DFG) and to Dr. M. Schiller from Chemson Polymer-Additive AG (Austria) for financial support of this work.

Moreover the authors acknowledge Prof. Dr. M. Buchmeiser and Dr. T. Scherzer from the Institute of Surface Modification (IOM, Leipzig) for giving the opportunity to perform photopolymerisation experiments using time-resolved IR spectroscopy.

Many thanks to Mrs. R. Müller from the Institute of Chemical Reaction Engineering of the University Erlangen-Nuremberg for doing powder XRD investigations.

## References

- [1] Tryk DA, Fujishima A, Honda K. *Electrochim Acta* 2000;45:2363.
- [2] Serpone N, Pelizzetti E, editors. *Photocatalysis, fundamentals and applications*. New York: Wiley; 1989.
- [3] Ollis DF, Al-Ekabi H, editors. *Photocatalytic purification and treatment of water and air*. Amsterdam: Elsevier; 1993.
- [4] Litter MI. Heterogeneous photocatalysis and transition metal ions in photocatalytic systems. *Appl Catal B Environ* 1999;23:89–114.
- [5] Troupis A, Hiskia A, Papaconstantinou E. Photocatalytic reduction – recovery of silver using polyoxometalates. *Appl Catal B Environ* 2003;42:305–15.
- [6] Rajeshwar K, Chenthamarakshan CR, Ming Y, Sun W. Cathodic photo-processes on titania films and in aqueous suspensions. *J Electroanal Chem* 2002;538–539:173–82.
- [7] (a) Abe R, Sayama K, Arakawa H. Dye-sensitized photocatalysts for efficient hydrogen production from aqueous  $I^-$  solution under visible light irradiation. *J Photochem Photobiol A Chem* 2004;166:115–22; (b) Abe R, Sayama K, Domen K, Arakawa H. A new type of water splitting system composed of two different  $TiO_2$  photocatalysts (anatase, rutile) and a  $IO_3^-/I^-$  shuttle redox mediator. *Chem Phys Lett* 2001;344:339–44.
- [8] Tammann G. About the influence of light on hardly soluble oxides in silver salt solutions. *Z Anorg Allgem Chem* 1920;114:151–2.
- [9] Arabatzis IM, Stergiopoulos T, Bernard MC, Labou D, Neophytides SG, Falaras P. Silver-modified titanium dioxide thin films for efficient photodegradation of methyl orange. *Appl Catal B Environ* 2003;42:187–201.
- [10] Sung-Suh HM, Choi JR, Hah HJ, Koo SM, Bae YC. Comparison of Ag deposition effects on the photocatalytic activity of nanoparticulate  $TiO_2$  under visible and UV light irradiation. *J Photochem Photobiol A Chem* 2004;163:37–44.
- [11] Senthilkumaar S, Porkodi K, Gomathi R, Geetha Maheswari A, Manonmani N. Sol–gel derived silver doped nanocrystalline titania catalysed photodegradation of methylene blue from aqueous solution. *Dyes Pigments* 2006;69:22–30.
- [12] Sclafani A, Mozzanega M-N, Pichat P. Effect of silver deposits on the photocatalytic activity of titanium dioxide samples for the dehydrogenation or oxidation of 2-propanol. *J Photochem Photobiol A Chem* 1991;59:181–9.
- [13] Keleher J, Bashant J, Heldt N, Johnson L, Li Y. Photo-catalytic preparation of silver-coated  $TiO_2$  particles for antimicrobial applications. *World J Microbiol Biotechnol* 2002;18:133–9.
- [14] Damm C, Sakthivel S, Kisch H. UV and visible light acrylate photopolymerisation initiated by nitrogen- or carbon-doped titanium dioxide. *Z Phys Chem* 2006;220:477–86.
- [15] (a) Damm C, Völtzke D, Abicht H-P, Israel G. Influence of the properties of  $TiO_2$  particles on a photocatalytic acrylate polymerisation. *J Photochem Photobiol A Chem* 2005;174:171–9; (b) Damm C. An acrylate polymerisation initiated by iron doped titanium dioxide. *J Photochem Photobiol A Chem* 2006;181:297–305; (c) Damm C, Herrmann R, Israel G, Müller FW. Acrylate photopolymerization on heterostructured  $TiO_2$  photocatalysts. *Dyes Pigments* 2007;74(2): 335–42.
- [16] Herrmann J-M. In: Baker RTK, Tauster SJ, Dumesic JA, editors. *Strong metal–support interactions*. ACS symposium series, vol. 298; 1986. p. 200–11.
- [17] Mueller FW, Damm C, Israel G. The role of traps in the interpretation of photo-EMF parameters of organic dye pigments. *J Inf Record* 2000;25: 533–52.
- [18] Israel G, Mueller FW, Damm C, Harenburg J. Measurement problems and kinetic treatment of photo-EMF curves. *J Inf Record* 1997;23: 559–84.
- [19] Scherzer T, Decker U. Kinetic investigations on UV-induced photopolymerization reactions by real-time FTIR-ATR spectroscopy: the efficiency of photoinitiators at 313 and 222 nm. *Nucl Instrum Methods Phys Res B* 1999;151:306–12.
- [20] Quinten M. The color of finely dispersed nanoparticles. *Appl Phys B Lasers Opt* 2001;73:317–26.